

# polymer papers

## Monitoring of reactive processing by remote mid infra-red spectroscopy

Jovan Mijović\* and Saša Andjelić

Department of Chemical Engineering, Polytechnic University, Six Metrotech Center, Brooklyn, NY 11201, USA

A novel experimental facility for remote mid infra-red (m.i.r.) spectroscopy has been assembled in our laboratory. We can conduct *in situ* real-time monitoring of practically any combination of processes and operating conditions, while, at the same time, enjoying the benefits of an unmatched wealth of molecular-level information contained in the m.i.r. range of the electromagnetic spectrum. The principal parts of our set-up are a host of optical components, gold-coated waveguides and a Fourier transform infra-red (FTi.r.) spectrophotometer. The signal generated in the remote mode was sharp, clear and reproducible, and the results were in every aspect as good as those obtained with conventional FTi.r. spectroscopy. The applicability of our remote m.i.r. set-up to *in situ* real-time monitoring of processing of reactive polymers was demonstrated by analysing the kinetics of cure of a multifunctional epoxy/amine formulation composed of diglycidylether of bisphenol-F (DGEBF) and 4,4'-methylene dianiline (MDA). A particularly interesting discovery was made concerning the necessary correction of the 'standard' epoxy peak at  $915\text{ cm}^{-1}$ , which must be considered in order to preserve the reliability of kinetic results in the later stages of cure. Copyright © 1996 Elsevier Science Ltd.

(Keywords: mid infra-red spectroscopy; reactive polymers; cure analysis)

### INTRODUCTION

*In situ* real-time monitoring of reactive processing of polymer-forming systems is of crucial importance to polymer scientists and engineers engaged in efforts to optimize processes and products. A remote monitoring set-up allows one to measure continuously changes in chemical and physical properties as they occur during processing in dies, moulds, reactors and autoclaves, at various pressures and temperatures. The sensed information is transmitted in real time to the computer, the task of which is to control the system parameters and guide the process along an optimum path.

Among various dielectric, acoustic and spectroscopic monitoring techniques, Fourier transform infra-red spectroscopy (FTi.r.) represents the most attractive choice owing to the unmatched wealth of molecular-level information contained in the infra-red portion of the electromagnetic spectrum<sup>1–6</sup>. But while the use of conventional (off-line) sample-compartment FTi.r. spectroscopy to study reactive polymers has been well documented in the literature<sup>7,8</sup>, the utilization of remote FTi.r. spectroscopy to monitor reactive processing has a recent origin.

Several reports on the use of remote near infra-red spectroscopy to study reactive polymeric systems have appeared in recent years<sup>9–11</sup>. The near infra-red range (or n.i.r.) extends from about  $14000$  to  $4000\text{ cm}^{-1}$  and contains weaker overtones of the fundamental absorptions. But the n.i.r. frequency range has one major

advantage in that it can be transmitted through silica-type optical fibres, which are relatively inexpensive and readily available in a variety of types and forms.

The mid infra-red range (or m.i.r.), which extends from about  $4000$  to  $400\text{ cm}^{-1}$ , is replete with fundamental absorptions and is richer in information, but it has a major disadvantage *vis-à-vis* the n.i.r. range in that only exotic and expensive chalcogenide and metal halide fibres have the required transmission capabilities at those frequencies, and even then usually over a limited interval<sup>12,13</sup>. It is therefore not surprising that only a few studies of remote m.i.r. spectroscopy have appeared in the literature, despite its potentially huge appeal.

In the pioneering work by Young *et al.*<sup>14</sup> on reactive polymers, an arsenic–germanium–selenium (As/Ge/Se) chalcogenide fibre was utilized to study the cure of a thermoset polyimide. The fibre had a core diameter of  $120\text{ }\mu\text{m}$ , an average attenuation of  $5\text{--}10\text{ dB m}^{-1}$ , and was capable of transmitting the m.i.r. signal in the  $5$  to  $9\text{ }\mu\text{m}$  range where several polyimide absorption peaks appear. A graphite fibre/polyimide (PMR 15) prepreg tape was also investigated by inserting the optical fibre through the prepreg sandwiched between a hot plate and an aluminium heating block. A small length of the fibre, stripped of cladding and exposed to the sample, acted as sensor element. The change in absorbance of imide bands at  $1710$  and  $1785\text{ cm}^{-1}$  was plotted as a function of time to demonstrate the monitoring ability of their experimental set-up, but no attempt was made to correlate this information with a fundamental kinetic model or to use it in a pilot-scale equipment for closed-loop process

\* To whom correspondence should be addressed

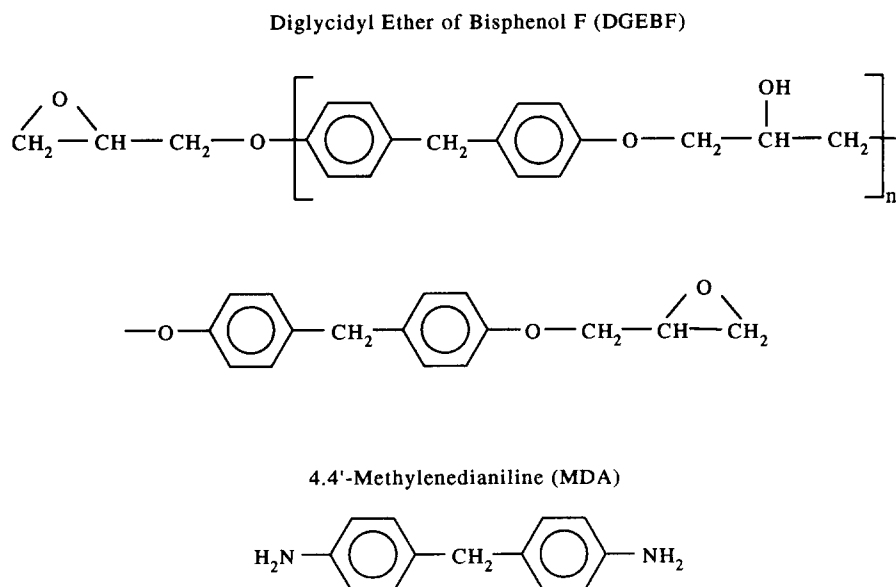


**Figure 1** Chemical structure of diglycidylether of bisphenol-F (DGEBF) and 4,4'-methylene dianiline (MDA)

control. Marand *et al.*<sup>15</sup> employed remote m.i.r. spectroscopy to study the cure of an epoxy/amine formulation composed of diglycidyl ether of bisphenol-A (DGEBA) and 4,4'-diaminodiphenyl sulfone (DDS). They utilized a 15-in long sapphire fibre but obtained few data points as their efforts were hampered by the cut-off frequency at  $2400\text{ cm}^{-1}$  and the problems with high cost and brittleness of the fibre.

In this paper we present an alternative approach to remote m.i.r. spectroscopy which utilizes gold-coated waveguides instead of fibre optics and which could be used for *in situ* real-time process control in practically any environment. The principal objectives of this paper are: (1) to describe a novel experimental set-up for remote m.i.r. spectroscopy recently assembled in our laboratory; and (2) to demonstrate the qualitative and quantitative analysis of our remote m.i.r. data using a multifunctional epoxy/amine formulation as an example.

## EXPERIMENTAL

### Materials

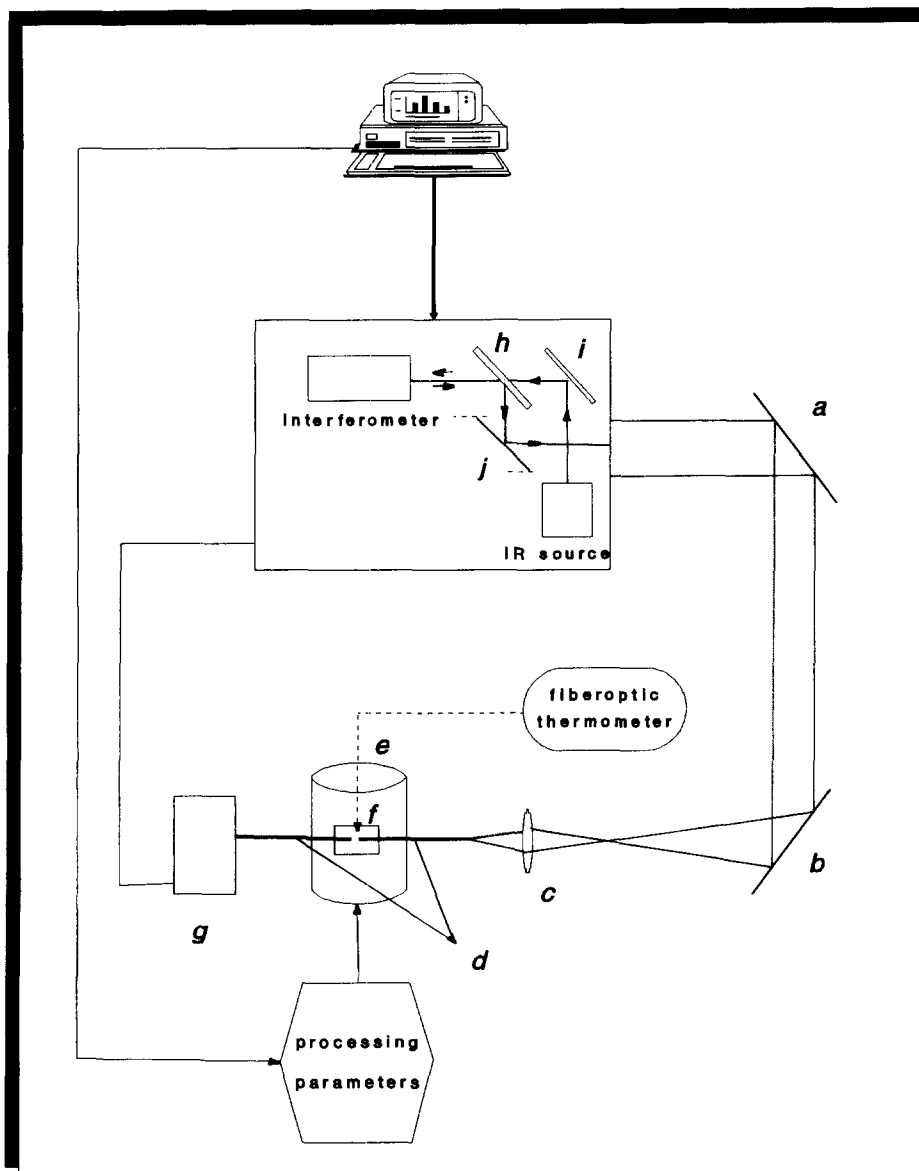
A multifunctional epoxy/amine formulation composed of diglycidyl ether of bisphenol-F (DGEBF) epoxy resin (Araldite PY 306, courtesy of Ciba-Geigy Corporation) and 4,4'-methylene dianiline (MDA, Aldrich) was used in this study. The chemical composition of the components is shown in *Figure 1*. The components were mixed in the stoichiometric ratio at room temperature and were then heated at  $70^\circ\text{C}$  for 10 min until a clear homogeneous solution was obtained. Samples were tested under isothermal conditions at a series of temperatures between 70 and  $100^\circ\text{C}$ . Prior to the introduction of reaction mixture into the reaction vessel, the latter was preheated to  $75^\circ\text{C}$  in order to minimize the lag in heat transfer due to conduction.

### Technique

*FTi.r.* was performed using Nicolet Magna-IR model 750 spectrometer operable in the spectral range from  $15800$  to  $50\text{ cm}^{-1}$  and a Vectra scanning interferometer capable of a better than  $0.1\text{ cm}^{-1}$  resolution. M.i.r. data

in the  $4000$  to  $600\text{ cm}^{-1}$  range were collected using an i.r. source, KBr beamsplitter and an MCT detector, which was cooled with liquid nitrogen before each run. All spectra were obtained at  $4\text{ cm}^{-1}$  resolution using 100 scans.

A schematic representation of our experimental set-up is shown in *Figure 2*. In order to conduct remote m.i.r. measurements, the i.r. beam had first to be directed out of the instrument. This was accomplished by placing a sliding mirror inside the optical bench compartment in the path of the beam near the exit from the interferometer. The sliding mirror is controlled by the computer and it can redirect the beam through the external ports on either side of the optical bench. Next, a series of optical components (for details see the key in *Figure 2*) was used to advance the beam a desired distance and focus it into a hollow nickel waveguide. The waveguide had an inside diameter of  $1.56\text{ mm}$  and was  $30\text{ cm}$  long. The inside was coated with gold, a highly i.r. reflective substance. Two identical waveguides were employed. During processing of samples that undergo cure, i.e. a transition from liquid to a crosslinked solid, the waveguides could be located in 'dummy' controls exposed to the identical thermal history as the main part, or in the parts that are subsequently machined off. Here, the waveguides were inserted into the reaction mixture through the holes drilled in the sides of the reaction vessel. A pair of NaCl windows ( $6\text{ mm}$  in diameter,  $1\text{ mm}$  thick) were attached to the end of each waveguide. The incoming i.r. beam advances down the receiving waveguide by internal reflection, travels through the sample where it collects the spectral information, and then proceeds down the transmitting waveguide by internal reflection towards the detector. The distance between the NaCl windows, and hence the sample thickness, is adjustable. Under the conditions of this study, the optimum absorption was obtained with a path length between  $200$  and  $500\text{ }\mu\text{m}$ . The MCT detector was removed from the optical bench compartment and placed immediately adjacent to the far end of the transmitting leg to minimize the loss of signal which was then processed by the *FTi.r.* computer.



## LEGEND :

- a** gold coated first surface flat mirror
- b** gold coated focusing mirror ( focal length = 760mm )
- c** ZnSe positive meniscus lens ( focal length = 62.5mm )
- d** nickel tubes ( 1 foot each, I.D. 1/16", gold coated inside ) with NaCl windows ( d=6mm,thickness=1mm ) bonded on each end
- e** reactor
- f** reaction vessel
- g** MCT ( liquid nitrogen cooled ) detector
- h** beamsplitter
- i** parabolic mirror
- j** sliding mirror

Figure 2 Schematic of experimental set-up for remote m.i.r. spectroscopy

Two different disposable reaction vessels were used in this study: polypropylene vessels (32 × 25 × 20 mm) for reaction temperatures up to approximately 130°C, and aluminium vessels for higher temperature. Heating

was accomplished by wrapping a rubber extruded heating tape around the reaction vessel. Temperature calibration was performed on non-reactive systems using Luxtron's 750 multichannel fiberoptic thermometer. The

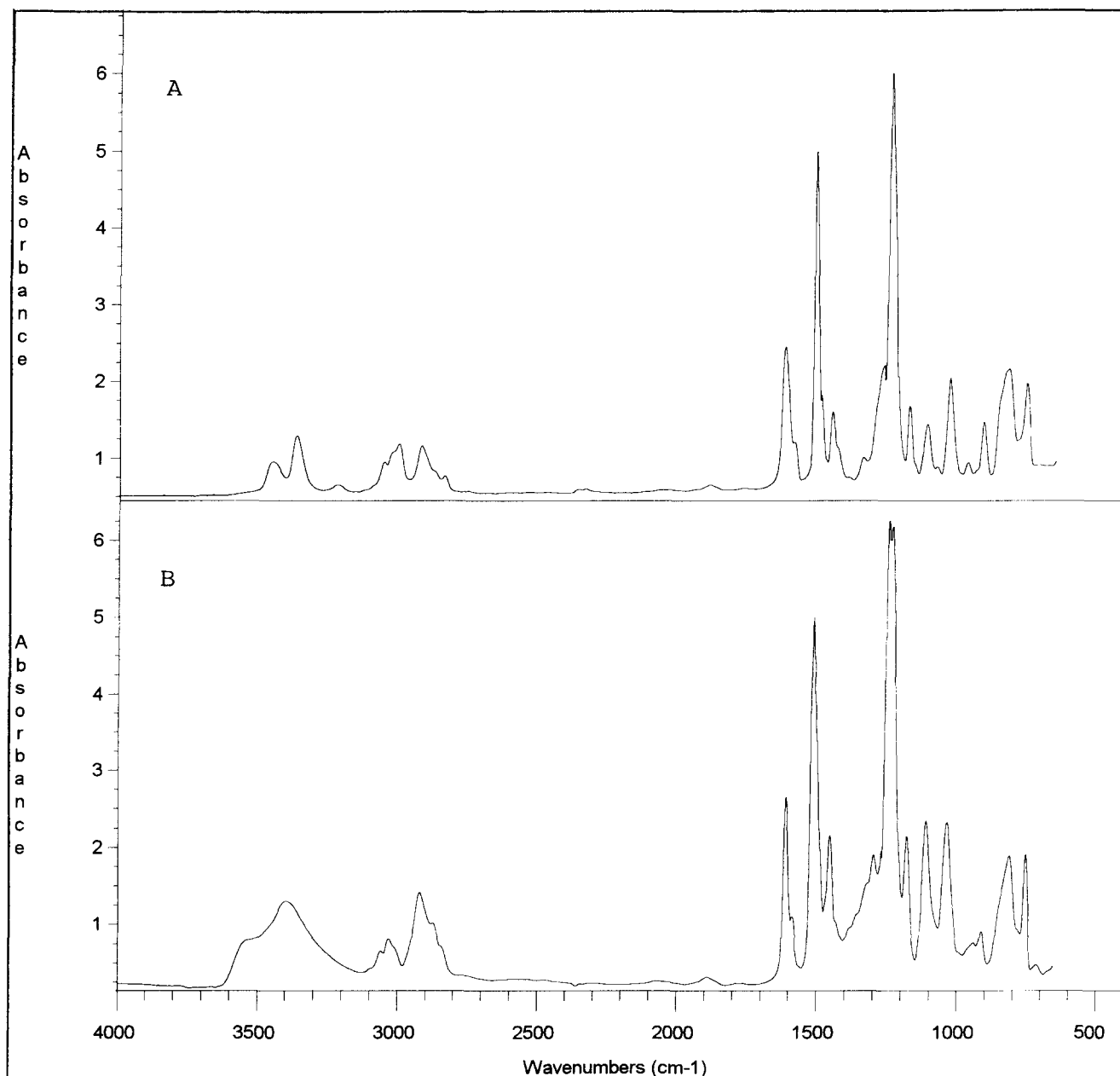


Figure 3 (A) M.i.r. spectrum of DGEBF/MDA formulation at the beginning of cure at 86°C; (B) m.i.r. spectrum of DGEBF/MDA formulation at the end of cure at 86°C

fibre-optic probe was immersed in the sample and its tip placed in the immediate vicinity of the space between the two NaCl windows. Stable isothermal conditions were achieved for all runs at all times. By maintaining the reaction vessel at cure temperature before injecting the sample, we were able to minimize the time lag due to conduction while reaching the processing temperature. A fine gauge Omega thermocouple was placed inside the sample to record the temperature during cure. Upon the completion of cure a short length of the exposed end of each waveguide was cut off with jeweller's saw and the new surface polished prior to the subsequent run.

We stress that the above-described remote m.i.r. set-up is novel, inexpensive (the price of disposable parts was about \$8 per experiment involving thermoset cure), versatile, and of potentially broad appeal since it can be utilized to generate *in situ* real-time m.i.r. spectra in

conjunction with practically any reactor and/or operating environment.

## RESULTS AND DISCUSSION

We begin our discussion by pointing out that sharp, reproducible spectra were obtained in the remote mode at all temperatures and stages of cure. It is important to emphasize that the clarity, reproducibility and reliability of spectra generated in the remote mode were in every aspect as good as the conventional (off-line) spectra obtained in the sample compartment of the spectrophotometer.

An example of a remote m.i.r. spectrum of the DGEBF/MDA formulation recorded at the very beginning of cure at 86°C is shown in *Figure 3A*. The following principal characteristic absorptions of epoxy/amine

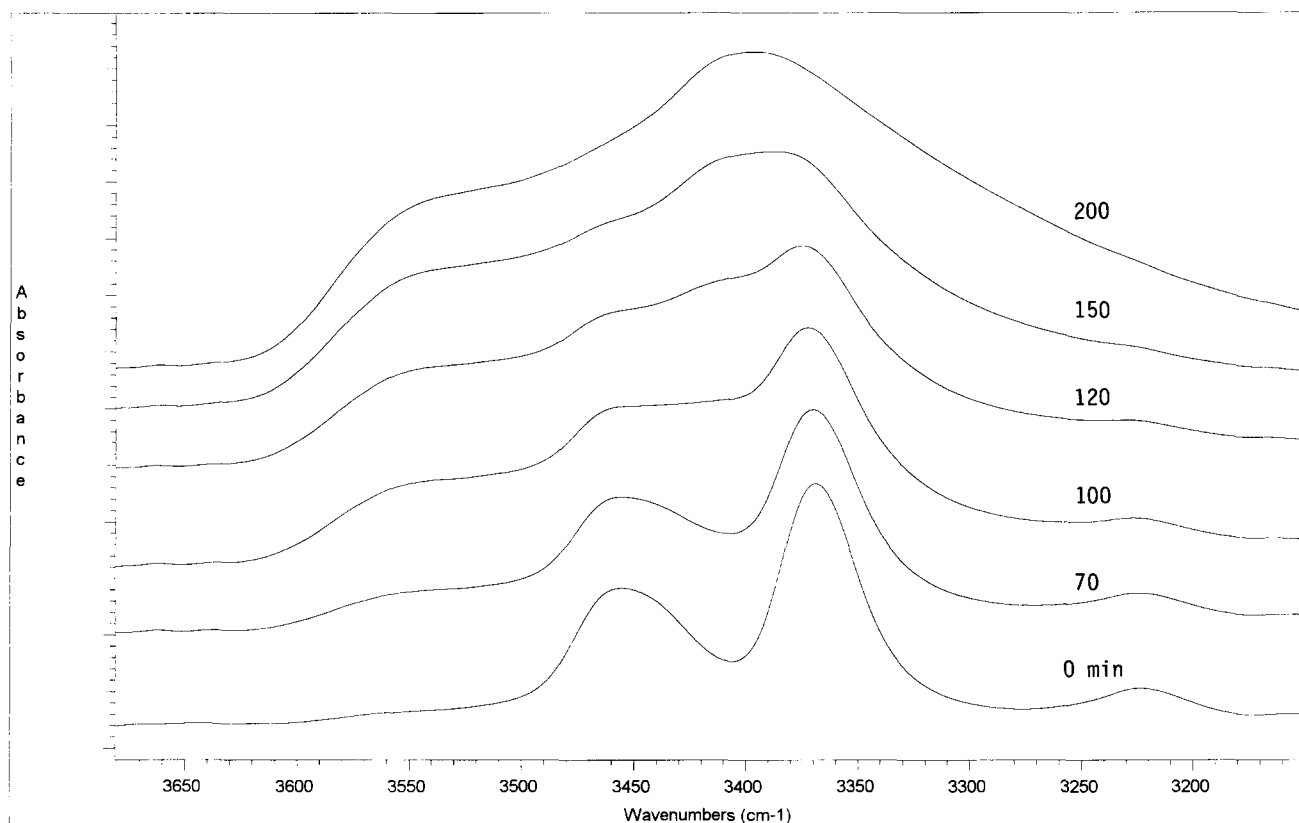


Figure 4 Enlarged view of changes in amine absorption peaks at 3360 and 3460  $\text{cm}^{-1}$  during 200 min of cure at 73°C

systems are noted. Absorptions at 3460 and 3370  $\text{cm}^{-1}$  are due to asymmetric and symmetric stretching vibrations, respectively, of the primary amine on the curing agent. A weaker absorption observed at 3225  $\text{cm}^{-1}$  was described earlier<sup>1</sup> as an overtone of the  $\text{NH}_2$  stretching band at 1630  $\text{cm}^{-1}$ , intensified by Fermi resonance due to its proximity to the stretching fundamentals. The  $\text{NH}_2$  absorption at 1630  $\text{cm}^{-1}$ , however, is overlapped by the benzene ring absorption. The N–H vibration of secondary amine appears at 3400  $\text{cm}^{-1}$  and can be distinguished from the absorption due to O–H stretching by spectral subtraction. The only 'visible' epoxy absorptions appear at 970 and 915  $\text{cm}^{-1}$ , with the latter commonly being used in quantitative studies of epoxy cure. Epoxy absorption also yields a two-shoulder peak near 840  $\text{cm}^{-1}$ , which is partially overlapped with out-of-plane hydrogen vibrations of *para*-disubstituted benzene rings. It is possible, however, to establish the presence of all 'hidden' epoxy absorptions by applying spectral subtraction at various intervals in the course of cure, as described later in the text. The ether group on the DGEBF molecule is characterized by three absorption peaks due to stretching vibrations at 1250, 1040 and 935  $\text{cm}^{-1}$ . The strong band at 1250  $\text{cm}^{-1}$  is due to aromatic carbon–oxygen stretching, while the band at 1040  $\text{cm}^{-1}$  results from aliphatic carbon–oxygen stretching (i.e. –O–CH<sub>2</sub>). The higher wavenumber shoulder of either peak at 1250  $\text{cm}^{-1}$ , which is noted at about 1300  $\text{cm}^{-1}$ , is the result of C–N stretching vibrations in aromatic primary amines.

In contrast to Figure 3A, which depicts the very onset of cure at 86°C, in Figure 3B we show the spectrum of a

sample that has reached the maximum degree of cure at that temperature. The most pronounced difference between Figures 3A and 3B concerns the increase in absorption due to the hydroxyl group, which is the product of reaction between epoxy groups and amine hydrogens. The peaks at 3560 and 3400  $\text{cm}^{-1}$  in Figure 3B are due to free and hydrogen-bonded–OH stretching absorption, respectively.

In Figures 3A and 3B we have established the origin of absorption peaks in the initial and final states of cure at an arbitrarily chosen temperature. Naturally, absorption intensities of all characteristic m.i.r. peaks undergo a systematic change in the course of cure; this is exemplified in Figures 4 and 5 which depict the first 200 min of cure at 73°C. Vertical shifts of different spectra in Figures 4 and 5, and in subsequent figures, were made for clarity. Figure 4 shows a gradual decrease in peaks of amine absorption due to symmetric and asymmetric stretching vibrations at 3370 and 3460  $\text{cm}^{-1}$ , respectively, as well as an increase in hydroxyl absorption around 3560 and 3400  $\text{cm}^{-1}$ . An enlarged view of the region of epoxy group absorption, which comprises peaks at 970 and 915  $\text{cm}^{-1}$ , is shown in Figure 5. Cure time and the corresponding extent of reaction are marked on each spectrum in the figure. At approximately 60% conversion, independent of cure temperature, we observed a shift in the epoxy absorption at 970  $\text{cm}^{-1}$  to lower wavenumber (i.e. lower frequency). Interestingly, the same phenomenon was observed in a non polymer-forming epoxy/amine model system and was reported in a previous communication from our group<sup>16</sup>. We believe that the underlying reason for this phenomenon is the

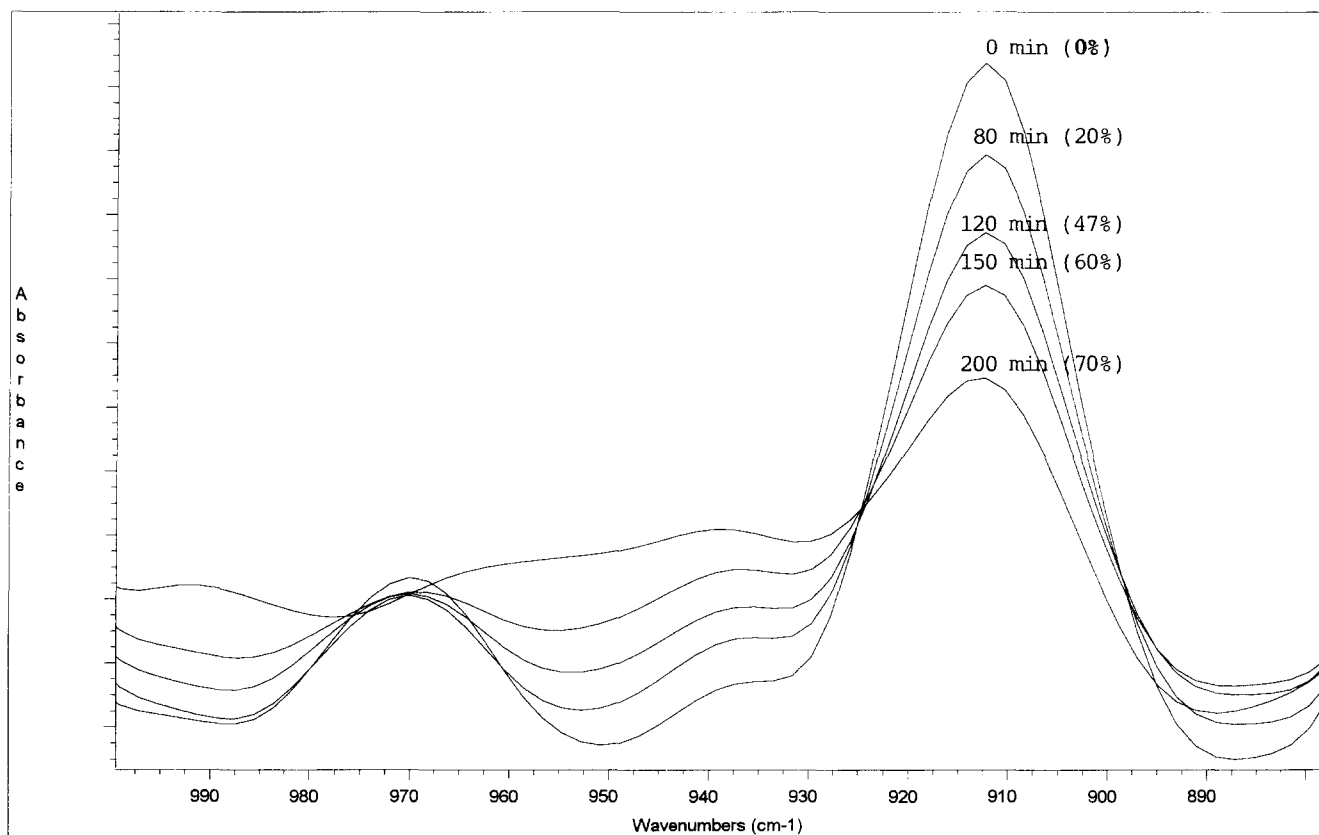


Figure 5 Enlarged view of changes in epoxy absorption peaks at 970 and 915  $\text{cm}^{-1}$  during 200 min of cure at 73°C

formation of additional bonding at this stage of reaction, which is enhanced by the simultaneous increase in the concentration of hydroxyl groups and viscosity. This is further discussed later in the text.

Epoxy/amine reaction kinetics were evaluated next. The extent of reaction ( $\alpha$ ) at any time  $t$  was calculated from the initial areas of epoxy and reference peaks,  $A_{\text{epoxy},0}$  and  $A_{\text{ref},0}$ , respectively, and their corresponding values at time  $t$ ,  $A_{\text{epoxy},t}$  and  $A_{\text{ref},t}$ , according to the following equation:

$$\alpha = 1 - [(A_{\text{epoxy},t}/A_{\text{ref},t})(A_{\text{epoxy},0}/A_{\text{ref},0})] \quad (1)$$

The peak at 915  $\text{cm}^{-1}$  was used to measure the disappearance of the epoxy group. Various reference peaks were examined and the most reproducible results were obtained using the peak at 2920  $\text{cm}^{-1}$  due to the  $-\text{CH}_2$  stretching vibration which did not vary during cure. The extent of reaction at 73, 86 and 100°C, calculated from equation (1), is plotted as a function of reaction time in Figure 6.

Further insight into the reaction mechanism was obtained by utilizing spectral subtractions at various stages of cure at a selected temperature. In Figures 7 and 8, which are presented separately for clarity, trace a was obtained by subtracting the spectra collected after 20 and 90 min of cure (corresponding to 10% and 59% conversion, respectively), while trace b was generated by subtracting the spectra collected after 90 and 180 min of cure, at which point, according to equation (1), a 76% conversion was attained and the reactions have ceased. Upward and downward pointing peaks in traces a and b reflect the appearance and disappearance, respectively,

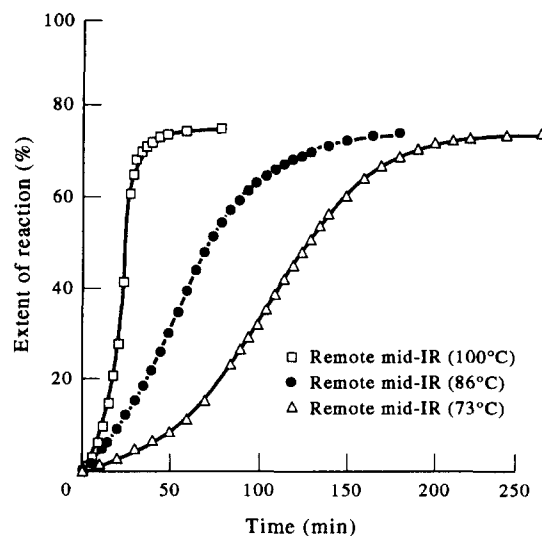


Figure 6 Extent of reaction as a function of cure time with cure temperature as a parameter

of absorption bands during reaction. Important information was extracted from this analysis. For instance, we were able to identify several relevant peaks in the region from 3600 to 2800  $\text{cm}^{-1}$  which were otherwise masked by the stronger neighbouring absorptions. By comparing traces a and b in that frequency range we were able to monitor trends in free and hydrogen-bonded hydroxyl absorptions during cure.

The most intriguing finding, however, concerns the observed difference in the rates at which various epoxy

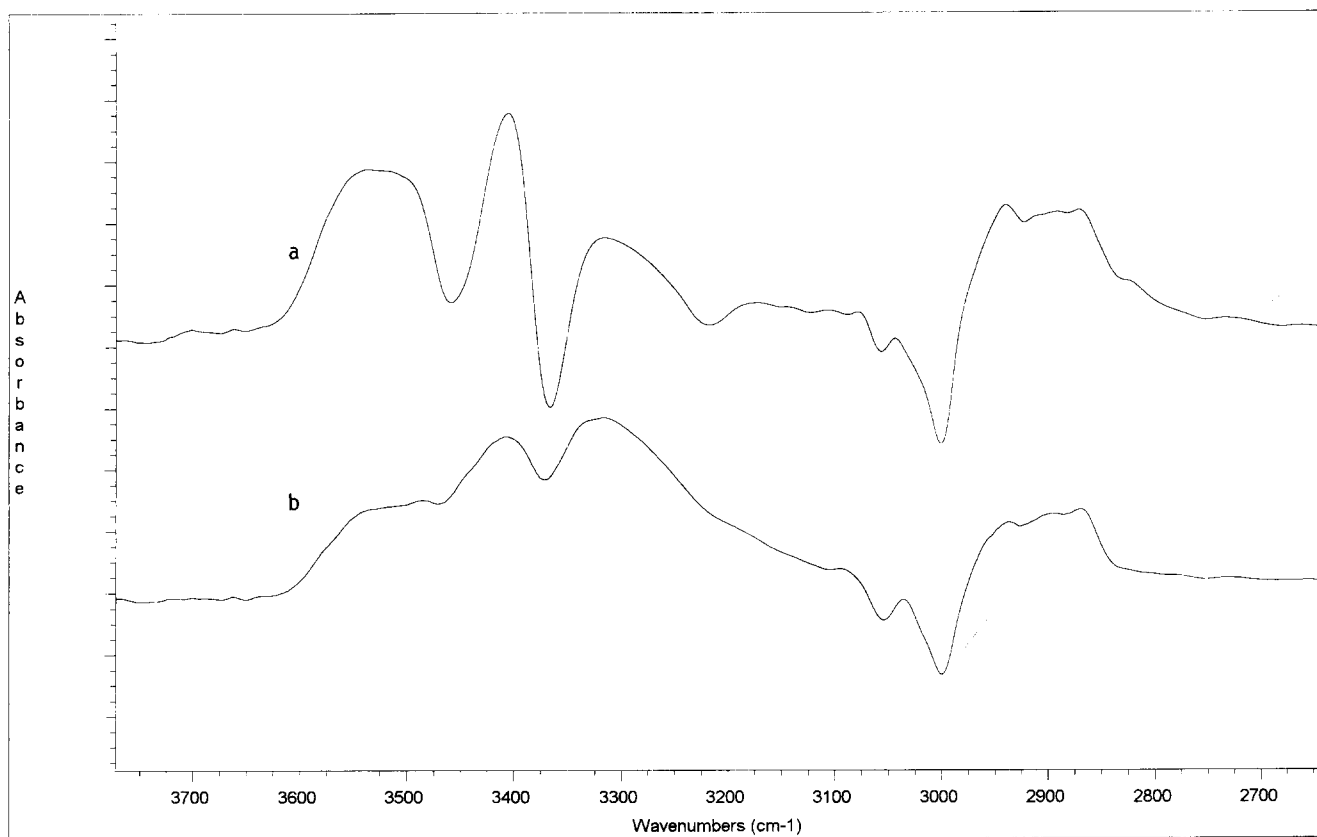


Figure 7 High wavenumber portions of difference spectra obtained during cure at 86°C: (a) between 20 and 90 min; (b) between 90 and 180 min

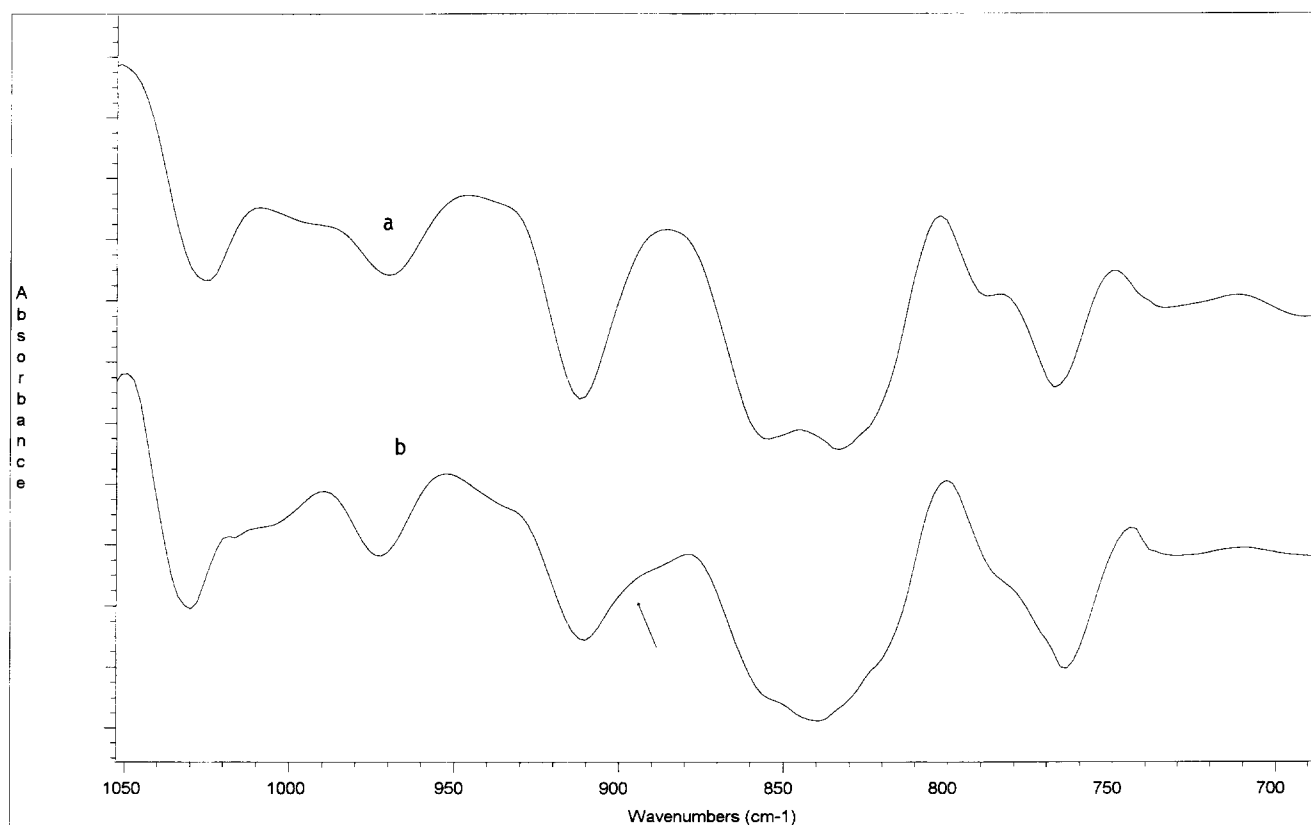


Figure 8 Low wavenumber portion of difference spectra obtained during cure at 86°C: (a) between 20 and 90 min; (b) between 90 and 180 min

absorptions decrease. We first analysed the areas under the previously 'hidden' epoxy peaks at  $3000\text{ cm}^{-1}$  and  $840\text{ cm}^{-1}$  and established that they decreased at identical rates. Surprisingly, however, the final conversion based upon those two peaks was approximately 15–16% higher than that based upon the 'standard'  $915\text{ cm}^{-1}$  peak, which is utilized almost exclusively in m.i.r. studies of epoxy/amine kinetics. An explanation for this observation was sought and is offered below based upon a comprehensive evaluation of a series of spectra. When different spectral subtraction intervals were examined, e.g. from 20 to 120 min (68% conversion) and 120 to 180 min, it became clear that the difference in absorption between  $915\text{ cm}^{-1}$  and other epoxy peaks increased gradually in the later stages of cure. Most interesting and fully reproducible changes were observed near  $900\text{ cm}^{-1}$  and above 60% conversion. Specifically, a new 'peak' near  $905\text{ cm}^{-1}$ , indicated by the arrow in Figure 8, began to emerge after about 60% conversion. We emphasize, however, that this new 'peak' can be seen only in the subtraction peaks and not in the standard spectra. The peak at  $970\text{ cm}^{-1}$  was not sharp enough for an accurate kinetic analysis. The emergence of the 'peak' near  $905\text{ cm}^{-1}$  was always observed at the same 'critical' conversion independent of temperature, suggesting a common molecular mechanism, namely gelation, which is known to occur in these systems in this conversion range<sup>17</sup>. We believe that the emergence and subsequent growth of this new peak immediately following gelation are a direct consequence of the network densification that is conducive to the formation of new complexes, the nature of which has been discussed in our earlier communications<sup>16,18</sup>. This discovery is always relevant to the studies of cure kinetics, since a continuing decrease in the epoxy peak at  $915\text{ cm}^{-1}$  used in kinetic calculations becomes masked by a simultaneous increase in the partially overlapping 'peak' at  $905\text{ cm}^{-1}$ , giving rise to a false slowdown and premature levelling off in the reaction rate. The most important consequence of the emergence of this new absorption at  $905\text{ cm}^{-1}$  is the necessity to take it into account in the quantitative analysis of epoxy/amine kinetics based upon the total area under the  $915\text{ cm}^{-1}$  peak, in order to avoid an (incorrect) underestimation of the degree of cure in the advanced stages of reaction. Otherwise, such kinetic results would have to be considered unreliable.

To check independently the validity of m.i.r. kinetics, the extent of our DGEBF/MDA formulation was next evaluated using an experimental set-up for remote fibre-optic near infra-red spectroscopy, which had been assembled in our laboratory earlier and was described elsewhere<sup>11</sup>. As in that study, we utilized the peak at  $4530\text{ cm}^{-1}$  to monitor the disappearance of epoxy groups and the peak due to C–H stretching vibration of the benzene ring at  $4673\text{ cm}^{-1}$  as a reference. The extent of reaction ( $\alpha$ ) at any time  $t$  was calculated from the initial areas of epoxy ( $4530\text{ cm}^{-1}$ ) and reference ( $4673\text{ cm}^{-1}$ ) peaks,  $A_{\text{epoxy},0}$  and  $A_{\text{ref},0}$ , respectively, and their corresponding values at time  $t$ ,  $A_{\text{epoxy},t}$  and  $A_{\text{ref},t}$  using equation (1). Extents of reaction of the DGEBF/MDA formulation at various temperatures calculated from n.i.r. and m.i.r. results are plotted together in Figure 9 for easy comparison. The minor discrepancy in the initial kinetic data obtained by the two techniques is accounted for by a thermal lag due to conduction in the m.i.r.

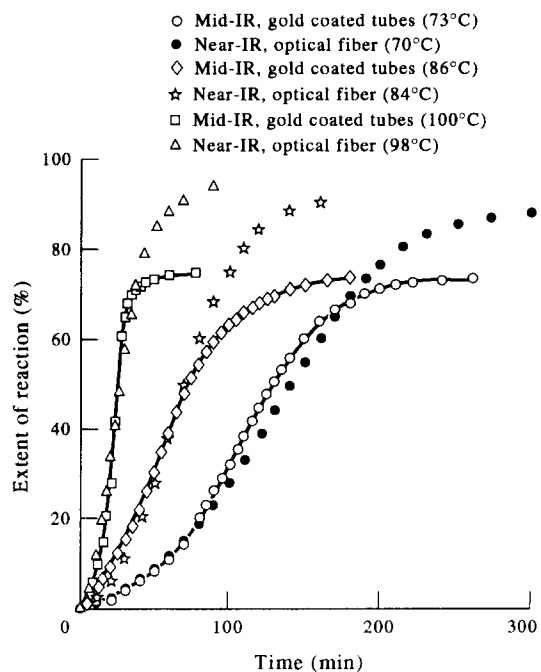


Figure 9 Extent of reaction as a function of cure time with cure temperature as a parameter calculated from m.i.r. and n.i.r. results

samples which is minimized in the capillary configuration of the n.i.r. samples. In general, however, excellent agreement between n.i.r. and m.i.r. kinetics is evident up to about 60% conversion, after which point the m.i.r. data quickly level off without exceeding 75% conversion. The accuracy and reproducibility of n.i.r. results are impeccable over the entire conversion range. The major discrepancy above that 'critical' conversion at  $\sim 60\%$  is caused by the emergence of the above-described new 'peak' at  $905\text{ cm}^{-1}$ , the growth of which gradually offsets the true decrease in the epoxy absorption at  $915\text{ cm}^{-1}$ . At present, however, we are not sure how to reconcile quantitatively and with high accuracy the opposite trends in peaks at  $915$  and  $905\text{ cm}^{-1}$  and how to incorporate that information in the kinetic calculations. We believe nonetheless, that a re-examination of a number of published studies of epoxy kinetics based on the  $915\text{ cm}^{-1}$  absorption (particularly in the later stages of cure) would be most informative and revealing.

## CONCLUSIONS

An experimental set-up for *in situ* real-time process monitoring by remote m.i.r. spectroscopy is now available in our laboratory. The infra-red beam is directed out of the spectrophotometer and advanced to a desired length and/or height by a series of optical components. The beam enters into the reactor through the receiving lag of a gold-coated hollow waveguide, passes through the sample, is transmitted to a MCT detector, and processed by the FTIR computer. The signal is sharp and highly reproducible, the set-up (apart from the spectrophotometer) is relatively inexpensive, and it can be adjusted for use with practically any processing vessel and/or operating conditions.

As an example, of the applicability of our set-up to monitoring of reactive polymer processing, we have conducted an investigation of cure of a multifunctional



epoxy/amine formulation. Intensities of characteristic absorption bands were monitored and used to evaluate the reaction kinetics. The most interesting finding in the kinetic study regards the emergence in the later stages of cure of a new absorption in the immediate vicinity of the standard epoxy peak at  $915\text{ cm}^{-1}$ , which must be handled appropriately to avoid unreliable kinetic results.

#### ACKNOWLEDGEMENTS

Part of this material is based upon work supported by the National Science Foundation under grant no. DMR-9400716. Funding for the purchase of the FTi.r. equipment provided by the Air Force Office of Scientific Research under grant #F49620-93-1-0603 is gratefully acknowledged. We are also grateful to Ad Boyer of Nicolet Instruments for his able and timely help with the experimental set-up.

#### REFERENCES

- 1 Colthup, N. B., Daly, L. H. and Wiberley, S. E. 'Introduction to Infrared and Raman Spectroscopy', Academic Press, New York, 1964
- 2 Griffiths, P. R. 'Chemical Infrared Fourier Transform Spectroscopy', Wiley, New York, 1975
- 3 Esposito, L. D. and Koenig, J. L. in 'Fourier Transform Infrared Spectroscopy' (Eds J. Ferraro and L. J. Basile), Academic Press, New York, 1978, Vol. 1
- 4 Ishida, H. (Ed.) 'Fourier Transform Infrared Characterization of Polymers', Plenum Press, New York, 1987
- 5 Spiro, I. J. and Schlessinger, M. 'Infrared Technology Fundamentals', Marcel Dekker, New York, 1989
- 6 Garton, A. 'Infrared Spectroscopy of Polymer Blends, Composites and Surfaces', Hanser, New York, 1992
- 7 Morgan, R. J. *Adv. Polym. Sci.* 1985, **72**, 1
- 8 Mertz, E. and Koenig, J. L. *Adv. Polym. Sci.* 1985, **75**, 73
- 9 George, G. A., Cole-Clark, P., St. John, N. and Friend, G. J. *Appl. Polym. Sci.* 1991, **42**, 643
- 10 St. John, N. and Geroge, G. A. *Polymer* 1992, **33**(13), 2679
- 11 Mijovic, J. and Andjelic, S. *Polymer* 1995, **36**, 3783
- 12 Simhony, S. and Katzir, A. *Appl. Phys. Lett.* 1985, **47**(12), 1241 and refs therein
- 13 Mijovic, J., Kenny, J. M., Nicolais, L. and Pejanovic, S. *SAMPE J.* 1992, **28**(5), 39 and refs therein
- 14 Young, P. R., Drury, M. A., Stevenson, W. A. and Compton, D.A.C. *SAMPE J.* 1989, **25**(2), 11
- 15 Marand, E., Baker, K. R. and Graybeal, J. D. *Macromolecules* 1992, **25**, 2243
- 16 Mijovic, J. and Andjelic, S. *Macromolecules* 1995, **28**, 2787
- 17 Mijovic, J., Kenny, J. M. and Nicolais, L. *Polymer* 1993 **34**(1), 207
- 18 Mijovic, J., Fishbain, A. and Wijaya, J. *Macromolecules* 1992, **25**, 979